Enhanced Quantum Sieving of Hydrogen Isotopes via Molecular Rearrangement of the Adsorbed Phase in Chabazite (Supporting Information)

Bastien Radola,[a] Igor Bezverkhyy,[a] Jean-Marc Simon,[a] José Marcos Salazar,[a] Mathieu Macaud,[b] and Jean-Pierre Bellat[a]

[a]*Laboratoire Interdisciplinaire Carnot de Bourgogne (ICB), UMR 6303 CNRS/Université de Bourgogne Franche-Comté, F-21078 Dijon, France*
[b]*CEA, DAM, Valduc, F-21120 Is-sur-Tille, France*

1 Experimental Methods

1.1 Sample Characterization

The sample of pure silica chabazite used in the present study was kindly provided by J. Patarin from IS2M laboratory (Mulhouse, France). The zeolite was prepared using the method described by Díaz Cabañas et al.[1]

XRD patterns of the solids were recorded in the range of 2-theta angle 3°–50° with a diffractometer Bruker D8-A25 Discover equipped with a LynxEye XE detector using Cu Kα radiation. The cell parameters were determined using the DICVOL software from the FullProf package. The N_2 adsorption–desorption isotherms were measured using a Micromeritics ASAP 2020 sorptometer at 77.4 K (under liquid N_2). The sample (~100 mg) was outgassed under secondary vacuum ($< 10^{-5}$ hPa) at 573 K overnight before measurements. The micropore volume was calculated from t-plot. The pore size distribution was calculated by the BJH method on the adsorption branch of the isotherm. SEM images were acquired using the scanning electron microscope JEOL 7600F. The sample was dispersed on a support coated with a conducting carbon tape and with an amorphous carbon layer of ~10 nm.

Figure S1 depicts the XRD patterns of our sample and the simulated one using the crystalline parameters reported by Díaz Cabañas et al.[1] It follows that their structures are identical to ours with only a minor difference in the cell parameters (see table S1). Data also show that the pore volume of our sample is lower by 16.7 %. N_2 adsorption–desorption isotherms (figure S2a) show a hysteresis suggesting the presence of mesopores whose volume is 0.05 $cm^3\,g^{-1}$ and whose size is in the 5–30 nm range (figure S2b).

Table S1: Structural and textural parameters of the pure silica chabazite used in this work.

	$a = b$ (Å)	c (Å)	Micropore volume ($cm^3\,g^{-1}$)	BET surface area ($m^2\,g^{-1}$)
Our sample	13.531	14.758	0.25	561
Díaz Cabañas et al.[1]	13.529	14.748	0.30	602

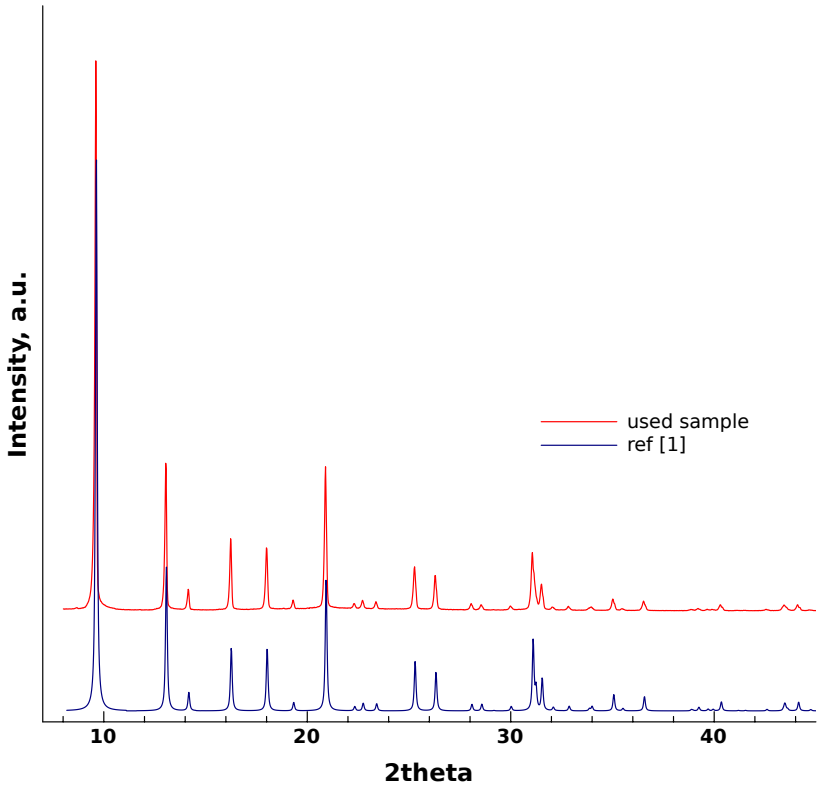

Figure S1: XRD pattern of our chabazite sample (red) and simulated XRD pattern with parameters given by Díaz Cabañas et al.[1] (blue).

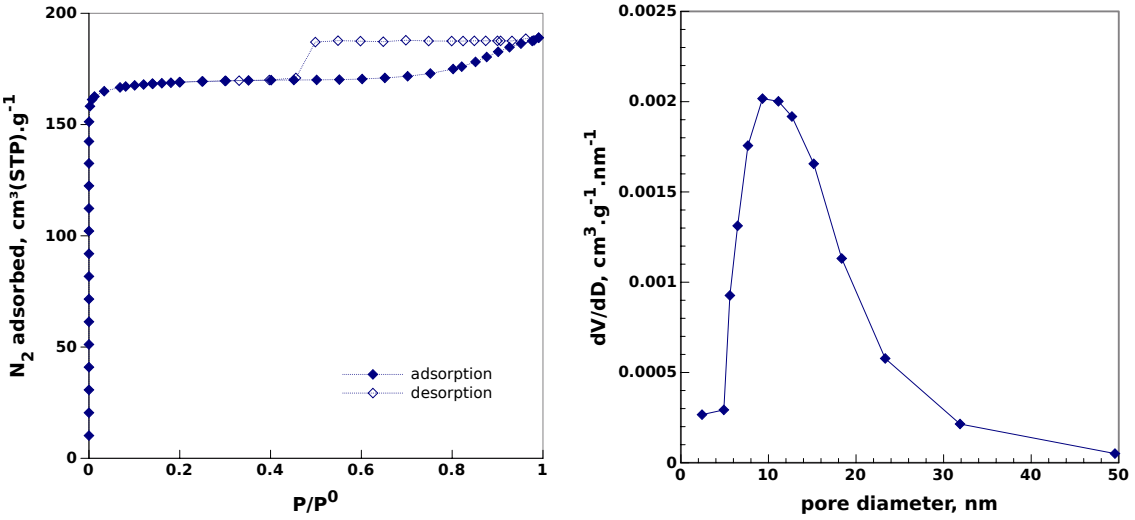

(a) N_2 adsorption–desorption isotherms.

(b) Pore size distribution.

Figure S2: Results of N_2 adsorption at 77.4 K in the chabazite used in this work.

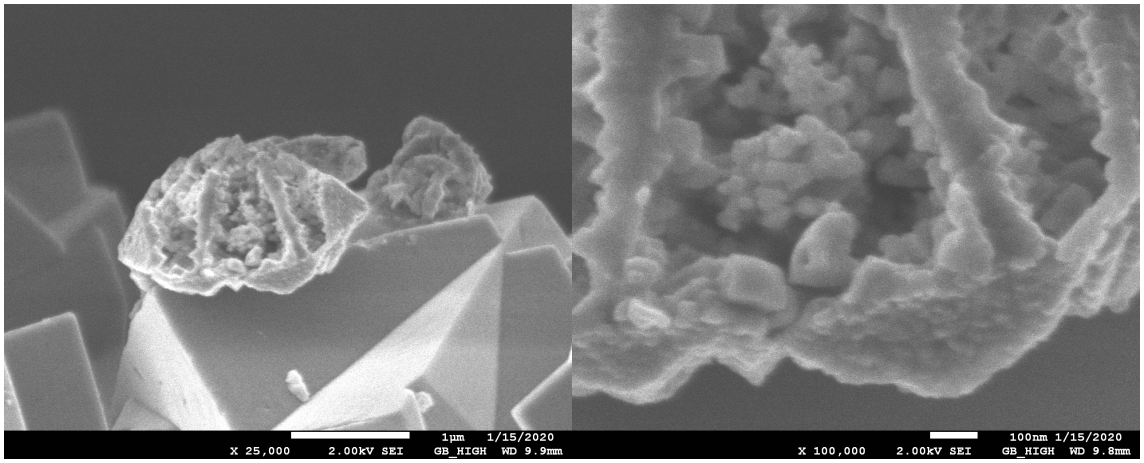

Figure S3: SEM images of the pure silica chabazite used in this work.

To understand the origin of the mesoporosity we characterized the sample by SEM. The sample consists mostly of well defined intergrown crystals of 3–5 µm but along with them some amorphous agglomerates can be observed (figure S3, left panel). They are composed of small particles of several dozens of nanometers and the size of the interparticle pores thus corresponds to the size of the observed mesopores (figure S3, right panel). The lower micropore volume of our chabazite can therefore be attributed to the presence of these amorphous agglomerates which do not contain micropores. The lower micropore volume of our sample distorts the comparison between the experimental and the simulated adsorption isotherms which were calculated for the ideal crystalline structure. Therefore, the experimental adsorbed amount of H_2 and D_2 was corrected by multiplying it by a factor of 1.2 (equal to the ratio of the micropore volumes).

1.2 H_2 and D_2 Single Gas Adsorption Isotherms

During adsorption and coadsorption measurements the temperature was maintained using a Gifford–McMahon He cryocooler from Micromeritics. In addition to the temperature measurement integrated in the cryostat, a silicon diode (DT-470 from Lake Shore Cryotronics) was placed directly on the measurement cell wall using the Kapton tape. It was found that the temperature measured on the cell wall was 1–5 K higher than the set point temperature depending on the temperature range. In the present work, the temperature measured by the diode was used as a reference. During the coadsorption measurements the cooled cavity of the cryostat in which the cell was placed was continuously purged with He.

Single gas adsorption isotherms were measured by means of the ASAP 2020 sorptometer from Micromeritics. The samples were degassed under secondary vacuum at 673 K for 16 h before the measurements. H_2 and D_2 gases used for these measurements were purchased from Air Liquide (France) and were additionally dried using zeolite filled cartridges from Agilent. The same gases were used for the coadsorption experiments.

1.3 Coadsorption Measurements

For coadsorption measurements a home built manometric setup was used, which was described in detail in our previous work.[2] The measurements were realized as follows. The sam-

ple was degassed under secondary vacuum at 673 K for 16 h, cooled to the room temperature under dynamic vacuum and placed into the cryostat at 90 K. When the desired temperature was reached (~3 h for 65 K and ~16 h for 40 K) the coadsorption experiment was performed according to the following procedure. First, the sample cell was isolated from the calibrated manifold volume which was filled with a 3:1 ratio H_2 + D_2 mixture by controlling the partial pressure of each gas. This initial mixture was equilibrated for 1 h which was found to be necessary to obtain a homogeneous mixture of H_2 and D_2. After homogenization time, the valve between the sample cell and the manifold volume was opened and the sample was kept in contact with the mixture until achieving equilibrium.

At the end of the equilibration period (16 h) the valve between the sample cell and the manifold volume was closed. Then, the adsorption capacity and selectivity were determined from a mass balance performed with the total pressure and the composition of the gas phase before and after adsorption. The gas mixture composition at equilibrium was determined with a mass spectrometer (Omnistar from Pfeiffer Vacuum) from the ratio of the surface areas of the peaks with $m/e = 2$ and 4. To determine the ratio of partial pressures of H_2 and D_2 from this data, the mass spectrometer should be calibrated. We found that reproducible results can be obtained only if the calibration is done after each measurement. Therefore, after the analysis of the equilibrium mixture, the manifold volume was evacuated and filled with a fresh 3:1 H_2 + D_2 mixture, which was then equilibrated for 1 h and analyzed. The response coefficient between the ratio of the pressures and the ratio of the peak areas thus measured was used to calculate the composition of the gas mixture obtained at equilibrium. Once all these measurements were done, the cryostat was replaced by a heating mantle, the sample was degassed at 673 K for 2 h and the described procedure was repeated again for another temperature.

In addition to a long equilibrium time, another important effect must be taken into account when measuring selectivity at low temperature: the thermal diffusion. This phenomenon results in the separation of two gases due to the temperature gradient existing between the manifold volume (at room temperature, ~295 K) and the sample cell (< 77 K). The thermal diffusion results in the enrichment of the cold volume with heavier species. In our case, this phenomenon was quantified using blank experiments performed in the same operation conditions (including the contact time of 16 h) but without any adsorbent. The selectivity thus obtained is due to the thermal diffusion and it can be expressed in the following way:

$$S_{\mathrm{TD}} = \frac{y_{\mathrm{D_2}}^{\mathrm{cold}} y_{\mathrm{H_2}}^{\mathrm{hot}}}{y_{\mathrm{D_2}}^{\mathrm{hot}} y_{\mathrm{H_2}}^{\mathrm{cold}}} \tag{1}$$

where y_i^{cold} and y_i^{hot} are the mole fractions of component i in the hot manifold and cold sample volumes. We found that in our setup the thermal diffusion selectivity is equal to 1.14 ± 0.05 when averaged over the range of pressure and temperature.

The effect of D_2/H_2 separation through the thermal diffusion should be subtracted from the values obtained with an adsorbent in order to obtain the true selectivity values related only to the adsorption-based separation. This was done using the following procedure. The molar fractions of H_2 and D_2 measured in the hot manifold volume (y_i^{hot}) were corrected in order to obtain the values existing in the cold sample cell (y_i^{cold}) by using the value of the measured selectivity of the thermal diffusion (S_{TD}). This can be done using the following equations derived from the definition of S_{TD} and taking into account that $y_{\mathrm{H_2}} + y_{\mathrm{D_2}} = 1$ for

Table S2: Crystalline parameters of the pure silica chabazite modeled in our simulations. The structure is hexagonal and one unit cell is composed of 36 Si atoms and 72 O atoms.

	$a = b$ (Å)	c (Å)	Pores width (Å)	Octagonal windows size (Å)
CHA	13.675	14.767	7.37	3.72

both cold and hot volumes:

$$y_{D_2}^{cold} = \frac{S_{TD} y_{D_2}^{hot}}{1 - y_{D_2}^{hot} + S_{TD} y_{D_2}^{hot}} \tag{2}$$

$$y_{H_2}^{cold} = 1 - y_{D_2}^{cold} \tag{3}$$

These corrected values of H_2 and D_2 fractions were then used to calculate the adsorbed amount of each species and the corrected adsorption selectivity:

$$\alpha_{D_2/H_2} = \frac{x_{D_2} y_{H_2}^{cold}}{y_{D_2}^{cold} x_{H_2}} \tag{4}$$

where x_i is the molar fraction of component i in the adsorbed phase.

All experimental values of D_2/H_2 selectivity reported in the present study are the corrected values calculated this way. Using repeated measurements we estimated that the relative standard error of the selectivity values is equal to 10 %.

It is worthy to note that our MS data rules out the possibility of the reaction of isotope exchange between H_2 and D_2.

2 Simulation Details

Grand canonical Monte Carlo simulations (GCMC) were done using the DL_MONTE[3,4] free software. The simulation box was built from 3×3×3 units cells of pure silica chabazite, whose crystalline parameters (table S2) and atomic positions were retrieved from the International Zeolite Association database.[5] The positions of the atoms inside the unit cell were relaxed by DFT calculations done using VASP, with the PBE-D3 exchange-correlation functional and dispersion corrections.

Isotope separation in nanoporous materials is governed by quantum effects arising at cryogenic temperatures (< 100 K).[6] The ideal method to deal with these effects is the path integral formalism, but its computational cost is prohibitive. In classical molecular simulations, a better suited approach is to use the Feynman-Hibbs potential:[7,8]

$$V_{GFH}(r_{ij}) = \left(\frac{6M_{ij}}{\pi\beta\hbar^2}\right)^{3/2} \iiint_{-\infty}^{+\infty} V(|\mathbf{r}_{ij} + \mathbf{u}|) e^{-u^2(6M_{ij}/\beta\hbar^2)} d\mathbf{u} \tag{5}$$

where $M_{ij} = m_i m_j (m_i + m_j)^{-1}$ is the reduced mass of the interacting particles, $\beta = (k_B T)^{-1}$, with k_B the Boltzmann constant, and $V(r_{ij})$ is the classical interaction potential. This method is based on the approximation of quantum particles as gaussian wave packets. By an expan-

Table S3: Lennard-Jones interaction parameters used in this work. Note that the parameters for D_2 are the same as the ones for H_2.

	ϵ_{ij}/k_B (K)	σ_{ij} (Å)
H_2-H_2	38.0	2.92
H_2-Si	39.0	2.80
H_2-O	47.0	3.08

sion of the integrand in powers of $\mathbf{r}$ up to the 4$^{\text{th}}$ order, we obtain:[9]

$$V_{\text{FH}}(r_{ij}) = V(r_{ij}) + \frac{\beta\hbar^2}{24M_{ij}}\left(\frac{2}{r_{ij}}\frac{\partial V(r_{ij})}{\partial r_{ij}} + \frac{\partial^2 V(r_{ij})}{\partial r_{ij}^2}\right) + \frac{1}{2}\left(\frac{\beta\hbar^2}{24M_{ij}}\right)^2\left(\frac{4}{r_{ij}}\frac{\partial^3 V(r_{ij})}{\partial r_{ij}^3} + \frac{\partial^4 V(r_{ij})}{\partial r_{ij}^4}\right) \tag{6}$$

with $V(r_{ij})$ usually chosen as the standard Lennard-Jones interaction potential:

$$V(r_{ij}) = 4\epsilon_{ij}\left(\left(\frac{\sigma_{ij}}{r_{ij}}\right)^{12} - \left(\frac{\sigma_{ij}}{r_{ij}}\right)^{6}\right) \tag{7}$$

of parameters ϵ_{ij} and σ_{ij}, respectively the well depth and the effective particle size. The 4$^{\text{th}}$ order development of the Feynman-Hibbs potential, which is accurate for confined fluids at cryogenic temperature,[10] was thus implemented in our copy of DL_MONTE.

H_2 and D_2 molecules were represented by a single sphere model (i.e., with only one van der Waals interaction site per molecule). The Lennard-Jones parameters used in this work are given in table S3. They have been carefully adjusted on experimental data for various pure silica zeolites. The full details of this procedure, which far exceed the scope of this communication, will be published in a forthcoming paper. The interaction cut-off radius was set to 15 Å. This parameter was optimized by analyzing the dependence of the configuration energy on its value. The zeolite framework was kept rigid during the simulations.

Simulations were done in the grand canonical ensemble μ, V, T. For convenience, we used the fugacity f instead of the chemical potential μ. Fugacity is related to pressure via the fugacity coefficient: $f = \phi p$. In this work, we considered the gaz phase to be ideal in our thermodynamic conditions ($T = 47$ K and $P \leq 100\,000$ Pa) and, thus, the fugacity is equivalent to the pressure (i.e., $\phi = 1$). This assumption was validated by calculating the fugacity coefficient of hydrogen using the data of Zhou et al.[11] This was further checked by simulations of single gases and mixtures in an empty box.

For single gases adsorption, 50 % translation moves and 50 % insertion–deletion moves were used. In the case of mixtures, only 45 % insertion–deletion moves were used, the remaining 5 % being converted to identity swap moves to speed up the equilibration. A number of 5 000 000 to 15 000 000 Monte Carlo cycles, depending on the pressure, was sufficient to reach equilibrium. Additional simulation cycles were then carried out for data analysis, which was done on up to 5000 configurations printed every 1000 cycles.

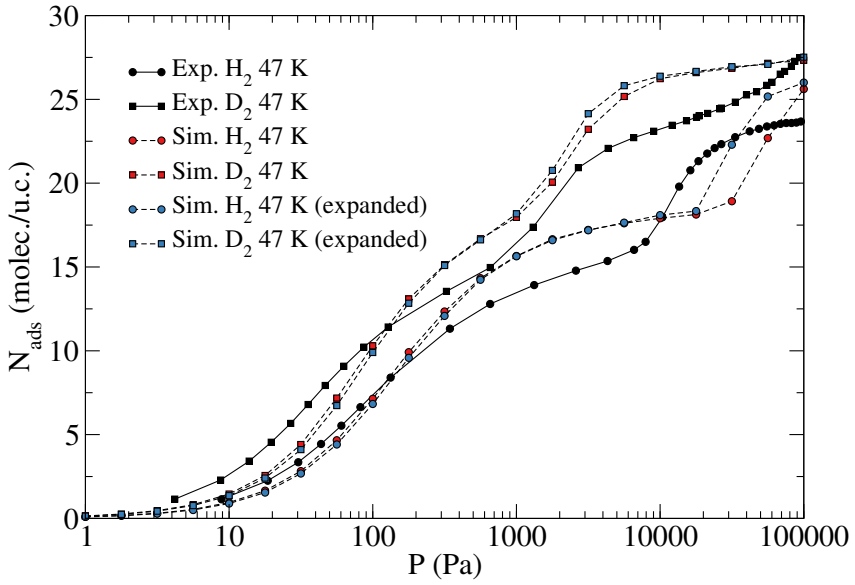

Figure S4: Experimental and simulated adsorption isotherms of single H_2 and D_2 in pure silica chabazite at 47 K. Simulations were done with a chabazite whose unit cell volume has been determined at room temperature and another whose unit cell parameters were expanded by 0.214 %.

3 Supplementary Results

The chabazite is known to have a large negative thermal expansion coefficient,[12] but its value has not been determined at temperatures below ambient conditions. Nonetheless, we carried out additional simulations to characterize the dependence of the apparition of a step in the adsorption isotherms on the unit cell volume of chabazite. To do this, we used the average thermal volume expansion coefficient measured in the 293–873 K range ($\overline{\alpha_V} = -26.1 \times 10^{-6}\,K^{-1}$) to extrapolate the chabazite volume at 47 K. This coefficient is defined as $\overline{\alpha_V} = \Delta V (V \Delta T)^{-1}$. Assuming for simplicity that the thermal expansion of chabazite is linear and isotropic, this corresponds to an expansion of the unit cell parameters by 0.214 %. Given the approximations we made, this value can by no means be considered realistic and is only a rough estimate. An expanded chabazite unit cell was thus built and the atomic positions were relaxed using DFT calculations. The GCMC results are given in figure S4. They show no dependence of the adsorption capacities on the unit cell volume. On the contrary, the step for H_2 shifts towards lower pressure values. This behavior is also visible for D_2 but it is much less pronounced. This modification of the adsorption isotherms enhances the agreement with the experimental data. Despite the rough estimate we used, it gives further confidence on the validity of our modeling.

In figure S5, we present some snapshots of a superposition of 5000 configurations at equilibrium. They can be seen as a probability density of adsorbed molecules inside the chabazite pores, although on a purely qualitative level. With these snapshots, we can see that the adsorbed phase arranges itself in a double ring around the cage centers. Each ring has 3 preferential adsorption sites, located in front of the octagonal windows before the step, and in front of the tetragonal windows after the step (see figure 3 of the main communication). This rearrangement is concomitant with the appearance of a new adsorption site at the window centers. This last point was already discussed in the main text with the help

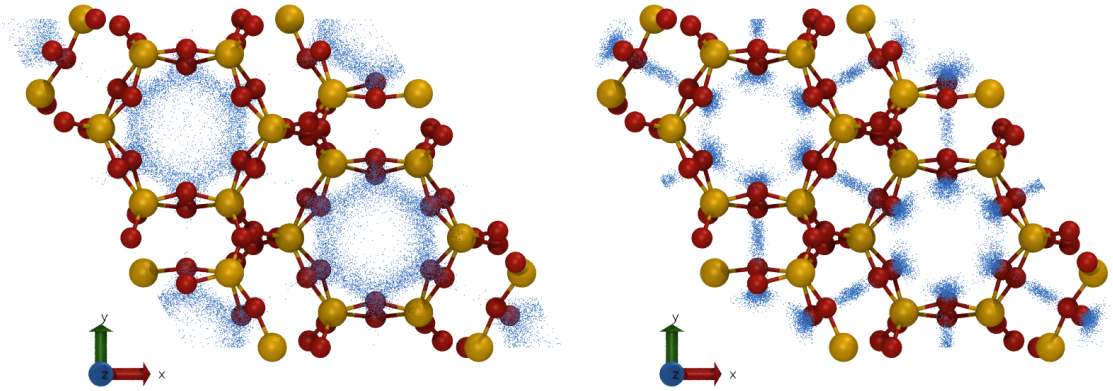

(a) $P = 316$ Pa (before the step).

(b) $P = 100\,000$ Pa (after the step).

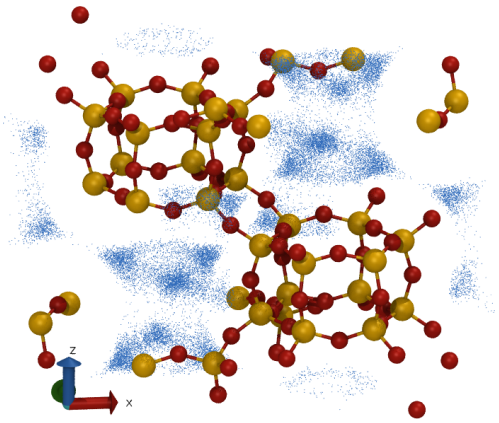

(c) $P = 316$ Pa (before the step).

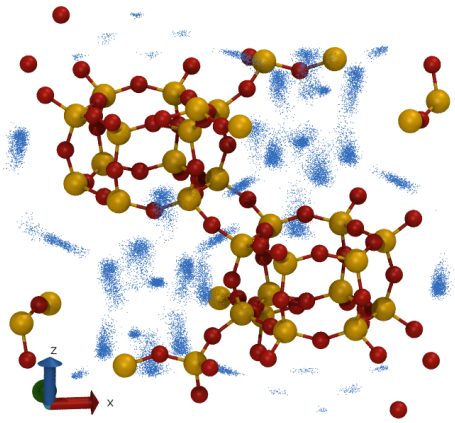

(d) $P = 100\,000$ Pa (after the step).

Figure S5: Snapshots of 5000 superposed configurations of H_2 molecules adsorbed in one unit cell of pure silica chabazite, viewed along two different directions both before and after the step. Oxygen and silicon atoms are represented in red and yellow, respectively, and hydrogen molecules in blue. The corresponding snapshots for D_2 are very similar and are thus not shown here.

of density profiles. Moreover, it can be seen that the adsorption sites have a smaller spatial extension after the step.

To characterize the last point on a more quantitative level, radial distribution functions are plotted in figure S6. They exhibit sharper peaks after the step, evidencing a denser adsorbed phase due to an increased confinement inside the chabazite pores. This is in full agreement with the analysis of the snapshots. Note that the position of the peaks for D_2 are slightly shifted towards lower distances compared to H_2. This corresponds to the modification of the effective molecular size due to quantum effects modeled by the Feynman-Hibbs potential.

References

(1) M. J. Díaz Cabañas and P. A. Barrett, *Chem. Commun.*, 1998, 1881–1882.

(2) M. Giraudet, I. Bezverkhyy, G. Weber, C. Dirand, M. Macaud and J.-P. Bellat, *Microporous Mesoporous Mater.*, 2018, **270**, 211–219.

(3) J. A. Purton, J. C. Crabtree and S. C. Parker, *Mol. Simul.*, 2013, **39**, 1240–1252.

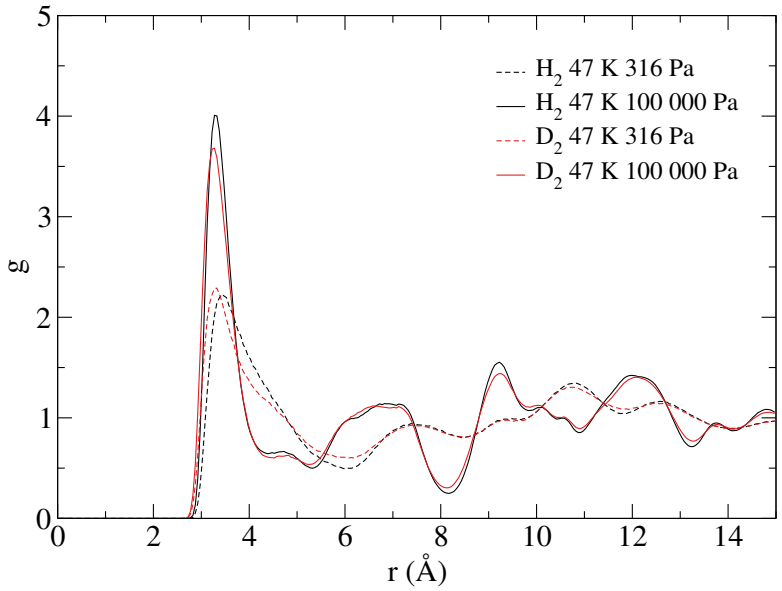

Figure S6: Pair radial distribution functions of adsorbed molecules in pure silica chabazite in the single gas adsorption case, both before the step ($P = 316$ Pa) and after ($P = 100\,000$ Pa).

(4) A. V. Brukhno, J. Grant, T. L. Underwood, K. Stratford, S. C. Parker, J. A. Purton and N. B. Wilding, *Mol. Simul.*, 2019, 1–21.

(5) *International Zeolite Association (IZA) database*, `http://www.iza-structure.org/databases/`.

(6) J. J. M. Beenakker, V. D. Borman and S. Y. Krylov, *Chem. Phys. Lett.*, 1995, **232**, 379–382.

(7) R. P. Feynman and A. R. Hibbs, *Quantum Mechanics and Path Integrals*, New York: Dover Publications, Inc., 1965, p. 365.

(8) L. M. Sesé, *Molec. Phys.*, 1994, **81**, 1297–1312.

(9) L. M. Sesé, *Molec. Phys.*, 1995, **85**, 931–947.

(10) A. V. A. Kumar, H. Jobic and S. K. Bhatia, *J. Phys. Chem. A*, 2006, **110**, 16666–16671.

(11) L. Zhou and Y. Zhou, *Int. J. Hydrogen Energ.*, 2001, **26**, 597–601.

(12) D. A. Woodcock and P. Lighfoot, *Chem. Mater.*, 1999, **11**, 2508–2514.